PHYSICAL REVIEW C **73**, 031601(R) (2006)

Nucleon-nucleon symmetry potential term and giant dipole resonance γ-ray emission

G. Giuliani and M. Papa*
Istituto Nazionale di Fisica Nucleare Sezione di Catania, Via Santa Sofia 64, I-95123, Italy
(Received 9 December 2005; published 14 March 2006)

A study of the dependence of the giant dipole resonance γ-ray yield from different functional forms of the symmetry term for the nucleon-nucleon interaction potential has been performed through the semiclassical molecular dynamics approach CoMD-II. We studied central and midperipheral reactions in the charge/mass asymmetric system $^{40}Ca + ^{48}Ca$ at 45 MeV/nucleon. The calculations show that the balance between the dynamical and the statistical emission is very sensitive to the "stiffness" of the symmetry term. This sensitivity could be highlighted by measuring the degree of coherence and the anisotropy ratio related to the dynamically emitted radiation.

DOI: 10.1103/PhysRevC.73.031601 PACS number(s): 25.70.−z, 21.30.Fe, 21.65.+f, 24.30.Cz

In recent years the study of the isospin dependence of the nuclear equation of state (EOS) at Fermi energies has triggered wide interest in the nuclear physics community. At a density far from the saturation value, the poorly known symmetry term [1] can strongly influence phenomena such as the evolution of supernovae and neutron stars [2] and can affect the structure of exotic nuclei [3,4]. An intense activity in this field has produced quite interesting results from the theoretical and experimental points of view. These results concern mostly the study of the behavior of hadronic probes produced through nucleus-nucleus collisions in which at least one of the two partners is a neutron-rich nucleus. The unusual charge/mass asymmetry ratio of a hot compound, obtained through the collision of nuclei (projectile and/or target) with a high neutron excess, can highlight the "stiffness" of the symmetry term. In particular, the scaling properties of the fragment isotopic and isotonic distributions, the differential neutron-proton flow and the degree of isospin diffusion have been considered for this purpose [5–15].

At the same time, starting from the first experiments reported in Refs. [16,17], it was shown that systems with a large difference in the charge/mass asymmetry between projectile and target can produce preequilibrium giant dipole resonance (GDR) emission. This was observed as an extra yield compared to the analogous charge/mass symmetric system. Other experiments have confirmed this observation in different systems and at incident energies between 8–25 MeV/nucleon in both central and midperipheral collisions [18–25]. For the $^{40}Ca + ^{48}Ca$ system, as discussed in Refs. [21,25], this preequilibrium yield can be directly related to the "isospin" equilibration mechanism leading to charge/mass equilibration.

The aim of this work is to investigate the sensitivity of the GDR γ-ray emission to the "stiffness" of the symmetry energy term for the $^{40}Ca + ^{48}Ca$ system at 45 MeV/nucleon. In a rather general way in fact we can expect that the GDR properties directly depend on the density functional form of the symmetry potential in the Steinwedel-Jensen mode [26]. This dependence clearly comes out by looking at the volume and surface terms of the droplet model potential energy [27]. In particular we try to highlight this sensitivity by studying the dynamics of the above-mentioned system and the GDR γ-ray emission mechanisms by means of the constrained molecular dynamical model CoMD-II [28]. Therefore, before showing our results, we briefly recall the main ingredients of the model and the basic criteria used for the description of the γ-ray emission.

In CoMD-II, the Pauli principle requirement and the conservation of the total angular momentum are satisfied by using impulsive forces generated according to constraining procedures. The dynamical calculations are done by using a Skyrme I effective interaction with a compressibility $K = 210$ MeV for the isospin-independent part of the N-body Hamiltonian $\mathcal{H}^0$ [28]. The nucleon-nucleon hard-core repulsive interaction was simulated by free nucleon-nucleon elastic processes having a 50-mb low-energy cutoff [28]. For the hard case (H) and the soft one (S), the isospin-dependent part H^τ describing the nucleon-nucleon interaction is expressed, in analogy to Refs. [5,29], as follows:

$$\mathcal{H}^{\tau,H(S)} = G^{H(S)}\mathcal{H}_0^\tau, \tag{1}$$

$$\mathcal{H}_0^\tau = \frac{e_0}{\rho_0}\sum_{i>j}\left(2\delta_{\tau_i,\tau_j} - 1\right)\rho_{i,j}, \tag{2}$$

where $\rho_{i,j}$ represents the overlap integral of the nucleon Gaussian phase-space distributions [5,28]; e_0 and ρ_0 were fixed at 28 MeV and 0.165 fm^{-3} (saturation density). The density-dependent factors for the H and S cases have the following form [28]:

$$G^H = \frac{2u}{u+1}, \quad G^S = u^{-1/2}, \tag{3}$$

$$u = \frac{\sum_{i>j}\rho_{i,j}}{\sum_{i>j}\rho_{i,j}^{\text{g.s.}}}. \tag{4}$$

The scaling factor in the definition of the u variable is referred to the ground-state (g.s.) configuration obtained for the impinging nuclei. Finally we note that, because of the Pauli principle constraint and to the energy minimization procedure needed to find the g.s. configuration [28], the isospin

*Electronic address: papa@ct.infn.it

density dependence of the Fermi motion is implicitly taken into account in the dynamics.

Several thousand events have been generated for the simulation of the collisions $^{40}Ca + ^{48}Ca$ and $^{44}Ca + ^{44}Ca$ (the reference system) at 45 MeV/nucleon and for different impact parameters. According to Refs. [21,25], from the simulation it is possible to evaluate event by event the dipolar signals $d\vec{V}^i/dt$, where $\vec{V}^i = \sum_k \vec{v}_k^i$ is the time derivative of the total dipole in center of mass (c.m.) of the total system and $\vec{v}_k^i$ are the proton velocities. For each impact parameter it is then possible to evaluate the related ensemble average $d\vec{V}/dt$ (which is zero for the reference system) and the fluctuation around it; $d\vec{V}^{f,i}/dt = d\vec{V}^i/dt - d\vec{V}\,dt$. According to the Larmor formula [21,30], the Fourier transform of $d\vec{V}/dt$ gives an evaluation of the γ-ray emission spectrum connected to the coherent or dynamical contribution $Y_D(E)$. At 25 MeV/nucleon for the system $^{40}Ca + ^{48}Ca$, it has been shown that this preequilibrium contribution [19,21,24,25] is responsible for the extra yield, observed in the γ-energy interval $E =$ 10–15 MeV, with respect to the charge/mass quasisymmetric system $^{40}Ca + ^{46}Ti$. The average yield associated with the fluctuating dipolar signals $d\vec{V}^{f,i}/dt$ is instead responsible for the yield produced through a statistical mechanism, including both the collective and noncollective (bremsstrahlung) contributions. At long time intervals it was shown that the collective contribution corresponds to the one described in the framework of the statistical model based on the compound nucleus picture in the local time equilibrium hypothesis [21].

We now illustrate the main results obtained for the $^{40}Ca + ^{48}Ca$ system at 45 MeV/nucleon incident energy using different options for the symmetry term, according to Eq. (3). In Fig. 1, as an example, we show the dynamical and statistical contributions Y_D and Y_S, for central ($b = 1$ fm)(bottom panels) and midperipheral reactions ($b = 6$ fm). The results have been obtained by analyzing the dipolar signals for a time interval of 500 fm/c. The calculations also show that the statistical contribution for the $^{40}Ca + ^{48}Ca$ system is, within 2%, equal to the contribution for the $^{44}Ca + ^{44}Ca$. This makes it reasonable to estimate Y_D experimentally by subtracting the yield obtained for the symmetric system (for which the dynamical contribution is zero) from the total γ-ray yield produced by the $^{40}Ca + ^{48}Ca$ system. Figure 1 shows that the soft and hard symmetry terms generate different contributions for both the dynamical and the statistical yields. In particular, the S case produces a statistical yield distribution centered at higher energies and showing a slightly larger width. The differences in the centroid and in the width values are larger for central collisions. They are of the order of 30 and 20%, respectively. The centroid-energy shift between the S and H cases is nevertheless responsible for differences of about 60% in yield around 20 MeV. At 30 MeV, where the bremsstrahlung mechanism starts to play a role, the difference decreases to 30%. In the same energy region the dynamical yield gives a higher contribution for central collision in the H case. This is shown in the inset of Fig. 1. For $b = 6$ fm the hard case shows also a higher yield in the region of the maximum around 10 MeV. To understand the origin of this behavior, in Fig. 2 we

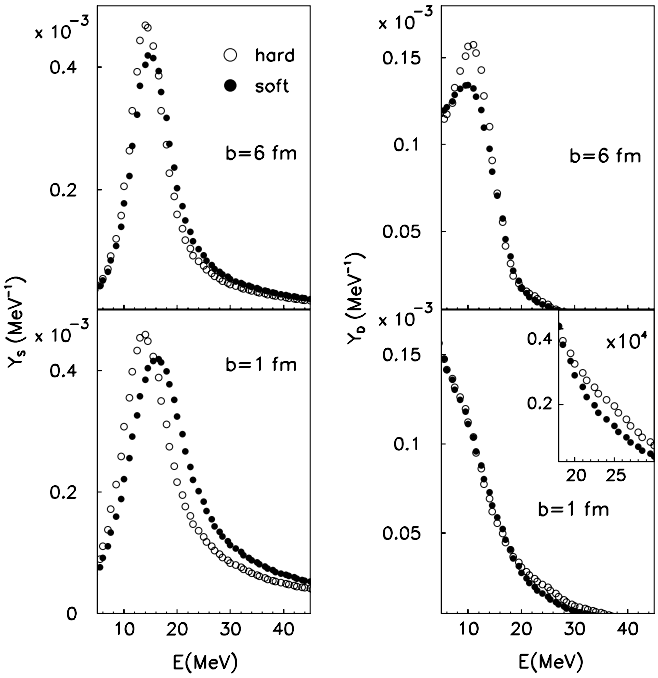

FIG. 1. Statistical, Y_S, and dynamical, Y_D, γ-ray yields evaluated for the $^{40}Ca + ^{48}Ca$ system at 45 MeV/nucleon for $b = 1$ fm and $b =$ 6 fm for the hard and soft cases. In the inset of the bottom-right panel the dynamical yield for central collisions is shown for γ-ray energy E between 18 and 30 MeV.

plot the time evolution of different quantities that can reveal the differences in the dynamics for $b = 1$ fm. In particular, in panel (a) we show the time evolution of the average mass number of the biggest fragment, A_1. This plot gives the time scale of the fragment formation process. For central collisions we obtain, on average, the multi-break-up of the hot compound with the three biggest fragments, A_1, A_2, and A_3, having a mass number of about 30, 18, 8 at 200 fm/c. From the figure we note that the first fragment is formed approximately in the time interval 70–120 fm/c. In Fig. 2(b) we show the average second time derivative of the total dipole along the beam axis $d\vec{V}_Z/dt = a_Z$. It determines the strength of the dynamical contribution. It is possible to note that, even if the S and H cases show the same quasiperiodicity, for the H case the slope of the signals is larger. This can explain, as a detailed Fourier analysis shows, the larger contribution to the coherent yield of the H case in the γ-energy region between 20 and 30 MeV (see the inset in Fig. 1). From a more microscopic point of view, this behavior can be related to the time dependence of the local density ρ_l as shown in Fig. 2(c); ρ_l was computed in the c.m. of the biggest fragment and it shows a faster change for the H case. From the figure we can see, in both cases, fast compression-decompression effects and the slower approach toward the normal density value after 100 fm/c. In particular, apart from the short time interval of about 20–30 fm/c that the system spends at density slightly higher than the normal one, the dynamics is dominated by the time evolution at lower density of the fragments produced. This implies that both the neutron single-particle potential V_s, plotted in Fig. 2(d),

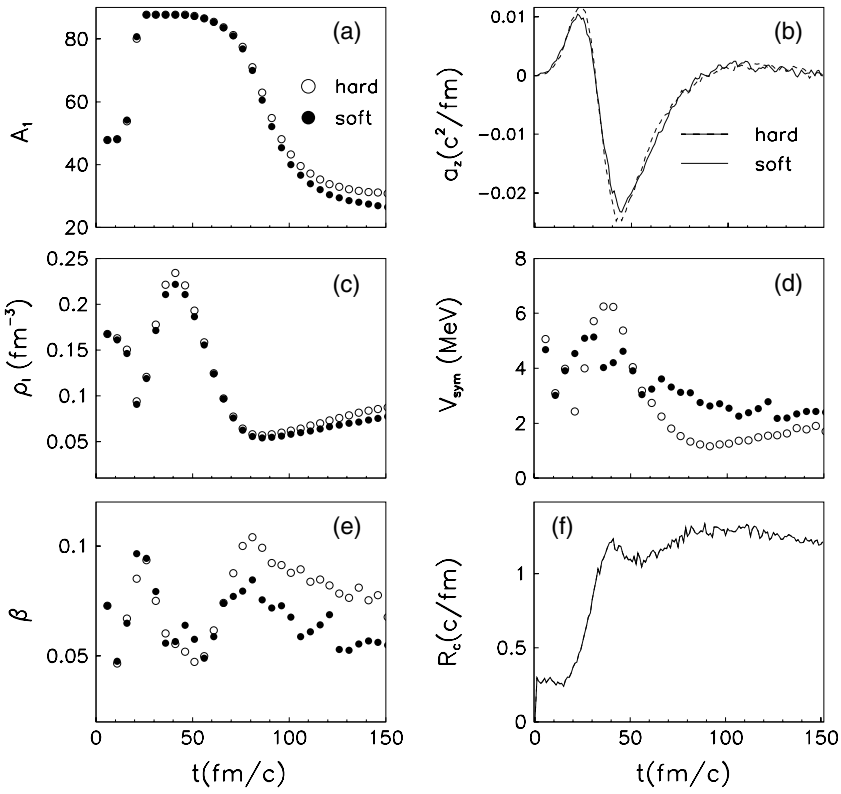

FIG. 2. For the $^{40}Ca + ^{48}Ca$ system at $b = 1$ fm and for the soft and hard cases, different average quantities are plotted as a function of time; (a) mass number of the biggest fragment A_1, b) second time derivative a_Z of the total dipole along the beam direction Z, (c) local density ρ_l evaluated in the c.m. of the largest fragment, (d) average single particle potential for the same fragment V_s, (e) related asymmetry parameter $\beta = (\rho_{l,n} - \rho_{l,p})/\rho_l$, (f) collision rate R_c.

and the related energy density W are higher for the S case during most part of the dynamical evolution. In particular, the W excess is about 1 MeV fm^{-3} in the time interval 50–150 fm/c and slowly decreases to about 0.4 MeV fm^{-3} at 500 fm/c. Therefore, as shown in Fig. 2(e), neutrons are emitted more easily for the soft EOS producing lower values of the $\beta = (\rho_{l,n} - \rho_{l,p})/\rho_l$ parameter for the largest fragments. This is also valid for the second biggest fragment. The above-mentioned differences at microscopic level also affect the collision rate R_c. Fragments that are poorer in neutrons

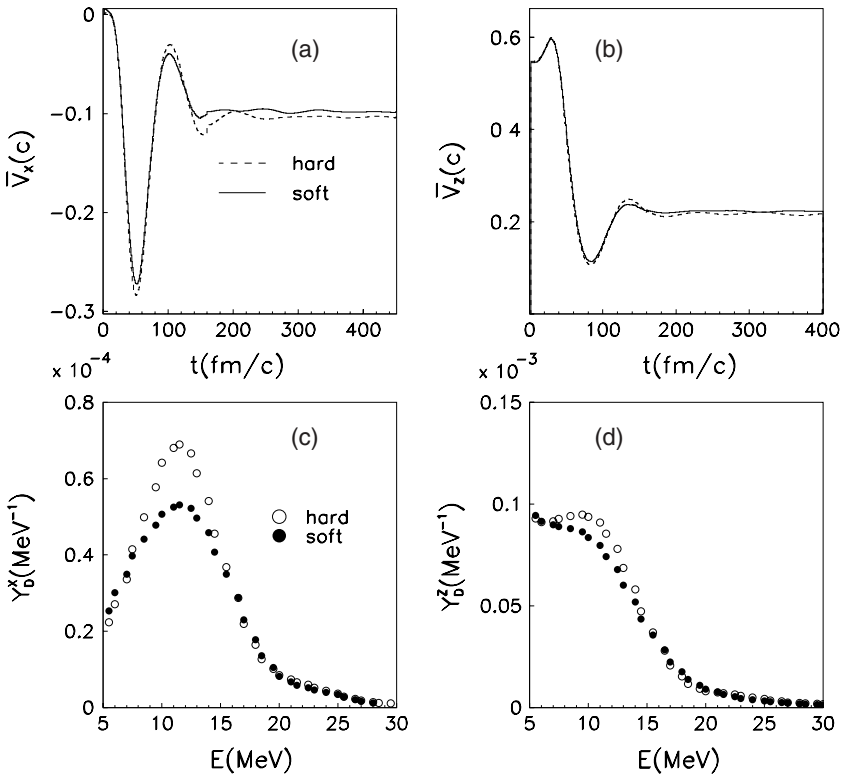

FIG. 3. For $b = 6$ fm (a) and (b) show the average time derivative of the total dipole along the impact parameter direction X and along the beam direction Z, respectively. In (c) and (d) the associated dynamical yields are also displayed.

and having an average value $Z/A < 0.5$, as obtained for the S case, produce a higher value of R_c as shown in Fig. 2(f). This is because of the increased relative number of neutron-proton collisions (having a higher cross section σ_{np}) and to the Pauli blocking factor that is less effective for low-energy neutron-proton collisions (the nucleon-nucleon cross section decreases with the energy).

The symmetry energy density W is proportional to the stiffness of the dipolar mode potential [26,27]. Therefore, in the S case, the larger values of W and R_c can explain the shift toward higher energies and the larger width of the statistical γ-ray yield produced in central collisions (see Fig. 1). The above scenario is also valid for midperipheral collisions, even if the differences concerning the statistical contribution are less marked because of the essential binary breakup of the system. In this case, however, as can be seen in Fig. 1 (upper panels), the most evident differences are related to the dynamical part. For midperipheral collisions, the nucleon-nucleon collision rate decreases by about 40% with respect to the central collisions so that less damping is obtained. The yield for the dynamical contribution is about 20% higher for the H case in the energy region around the maximum. In Fig. 3 we show calculations for $b = 6$ fm. Contrary to the central case, the excitation of the dynamical contribution $\overline{V_X}$ along the impact parameter direction starts to play a role (the average contribution along the Y direction is zero for symmetry reasons). The difference in the amplitude of oscillations is more evident for the X component with respect to the Z one. In fact, the X component behavior generates a yield difference of the order of 30% at 12 MeV, whereas the one associated to $\overline{V_Z}$ is about 10% at the same energy [see Figs. 3(c) and 3(b)]. This higher sensitivity of $\overline{V_X}$ with respect to $\overline{V_Z}$ can be linked to the lower effectiveness of the Pauli blocking for nucleon-nucleon collisions along the transverse direction.

Up to now we have discussed the relative dependence of the statistical and dynamical yields from the stiffness of the EOS symmetry term. In the following we will show the behavior of two observables related to these effects that can better highlight the above differences. These observables should be defined in such a way that their predicted numerical values show a weak or no dependence on the finite time of calculations. Moreover, it should be preferable, if possible, to eliminate in the definition some trivial dependence related to some detail of the calculations. In the first four panels of Fig. 4 we show the normalized degree of coherence $\Phi'_{\rm ch}(E) = \Phi_{\rm ch}(E)/\Phi_{\rm ch}(E_0)$ computed at different times t_s. The degree of coherence was introduced in Refs. [21,25]. It can be defined as follows:

$$\Phi_{\rm ch}(E) \equiv \frac{Y_D(E)}{Y_S(E) + Y_D(E)}. \tag{5}$$

We have chosen in this case the reference energy $E_0 = 11$ MeV. The calculations in fact show that $\Phi_{\rm ch}(E_0) \simeq 0.4$, almost independently from the stiffness of the symmetry term. The degree of coherence is determined practically by the relative yield of the dynamical γ-ray emission with respect to the statistical one; it is therefore a measure of the entrance channel memory for the charge/mass asymmetric system. It allows an expression of the model prediction in relative units, therefore eliminating some peculiar dependence related to the method used to estimate the radiative yield (application of the Larmor formula in a semiclassical first-order approximation). It weakly depends on time as can be seen by comparing the results shown in the panels (a) and (c) and, especially, (b) and (d). Between 20 and 30 MeV the sensitivity of $\Phi'_{\rm ch}$ to the different symmetry terms is rather high, both in the value and in the shape. This is because of two combined effects. In fact, in this energy range, the H case shows a larger dynamical yield and a smaller statistical contribution with respect to the S case (see Fig. 1). In Fig. 4(e), to have a more comprehensive picture, we show the value $\Phi'^{m}_{\rm ch}$ of $\Phi'_{\rm ch}$ computed at 21 MeV for $t_s = 500$ fm/c at different impact parameters for both S and H cases.

In Fig. 4(f) we display another observable, R^L_γ, which we call the anisotropy ratio. It is defined from the following quantity:

$$\alpha^L_\gamma = P(\theta, E)/Y^0_D,$$

where $P(\theta, E) = \frac{dY_D(\theta,E)}{d\theta}$ is the c.m. angular distribution of the dynamical γ-ray emitted at the angle θ with respect to the beam direction for midperipheral reactions and Y^0_D is the dynamical yield measured for central collisions; it very weakly depends on the symmetry potential in the energy interval

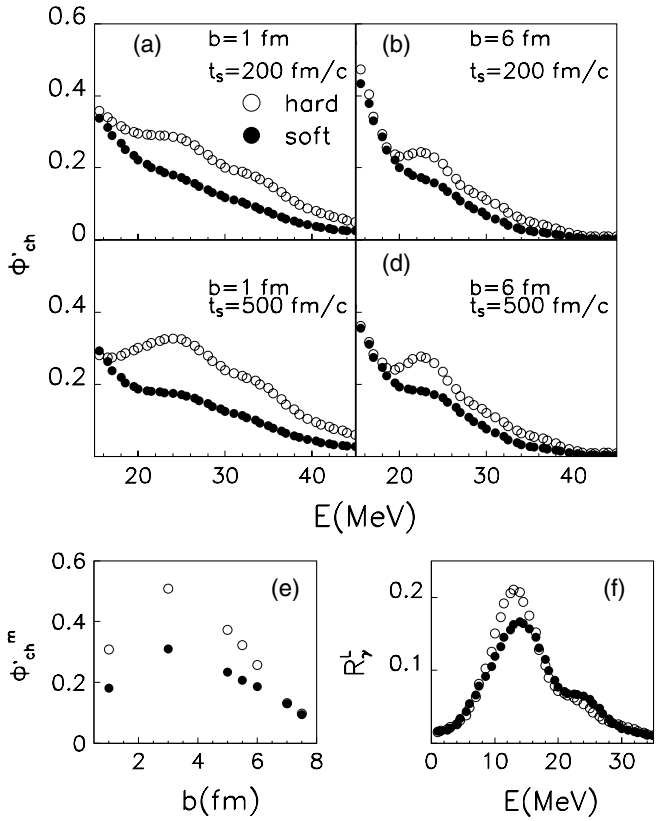

FIG. 4. In the first four panels [from (a) to (c)] the normalized degree of coherence $\Phi'_{\rm ch}$ is plotted as a function of the γ-ray energy E for $b = 1$ fm and $b = 6$ fm, for different calculation times t_S, for the soft (closed circles) and hard case (open circles). In (e) the value $\Phi'^{m}_{\rm ch}$ (see text) of $\Phi'_{\rm ch}$ computed at different impact parameters is also shown. In (f) we display R^L_γ(see text) as a function of E for the H and S cases.

between 10 and 15 MeV and is practically determined by the Z component of the dipolar signal. It can be easily shown that at very forward or backward angles ($\theta < 15^0$ or $\theta > 165^0$) $\alpha_\gamma^L \simeq R_\gamma^L = AY_D^X/Y_D^0$ within a few percentages A is a constant related to the total efficiency of the γ-ray detection apparatus. The main idea underlying the definition in the previous expression is to highlight the contribution related to the dynamical yield emitted by the dipolar signals along the impact parameter direction. As seen in Fig. 3, it shows the higher sensitivity to the stiffness of the symmetry term around 12 MeV. In particular, around 12 MeV the H case displays an anisotropy ratio that is about 30% higher than the value obtained for the S case. Finally we observe that, because R_γ^L involves only dynamical contributions, it is invariant with respect to later statistical processes.

In summary we analyzed, in a full N-body dynamical approach, the dependence of the dipolar radiative process from the stiffness of nucleon-nucleon symmetry potential for charge/mass asymmetry collision at 45 MeV/nucleon. Our results show that in the γ-ray energy region dominated by GDR emission, the interplay between dynamical emission, obtained through the study of a system such as the $^{40}\mathrm{Ca} + {}^{48}\mathrm{Ca}$ one and the statistical emission, is very sensitive to the density functional forms of the symmetry term in the low-density region. Moreover, we showed that the differences obtained can be highlighted by measuring two properly defined observables: The degree of coherence and the anisotropy ratio. We think that these kind of studies could integrate and be usefully compared with the results obtained from the observation of hadronic probes. This can give further information for the constraint the EOS of asymmetric nuclear matter.

We thank Dr. L. Lo Monaco and Dr. J. Winfield for the kind help with the text revision.

[1] *Isospin Physics in Heavy Ion Collision at Intermediate Energies*, edited by Bao-An Li and W. Udo Schroder (Nova Science Publisher, Inc., New York, 2001).
[2] J. M. Lattimer and M. Prakash, Astrophys. J. **550**, 426 (2001); Science **304**, 536 (2004).
[3] B. A. Brown, Phys. Rev. Lett. **85**, 5296 (2000).
[4] R. J. Furnstahl, Nucl. Phys. **A706**, 85 (2002).
[5] B. A. Li, C. M. Ko, and Z. Ren, Phys. Rev. Lett. **78**, 1644 (1997).
[6] V. Baran, M. Colonna, M. Di Toro, and A. B. Larinov, Nucl. Phys. **A632**, 287 (1998).
[7] H. S. Xu *et al*., Phys. Rev. Lett. **85**, 716 (2000).
[8] W. P. Tan *et al*., Phys. Rev. C **64**, 051901(R) (2001).
[9] V. Baran, M. Colonna, M. Di Toro, V. Greco, M. Zielinska-Pfabe', and H. H. Wolter, Nucl. Phys. **A703**, 603 (2002).
[10] M. B. Tsang, W. A. Friedman, C. K. Gelbke, W. G. Lynch, G. Verde, and H. Xu, Phys. Rev. Lett. **86**, 5023 (2001).
[11] B. A. Li, Phys. Rev. Lett. **85**, 4221 (2000).
[12] B. A. Li, Phys. Rev. Lett. **88**, 192701 (2002).
[13] L. Shi and Danielewicz, Phys. Rev. C **68**, 064604 (2003).
[14] B. A. Li, Phys. Rev. C **69**, 034614 (2004).
[15] L. W. Chen, C. M. Ko, and B. A. Li, Phys. Rev. Lett. **94**, 032701 (2005).
[16] S. Flibotte *et al*., Phys. Rev. Lett. **77**, 1448 (1996) and reference therein.
[17] L. Campaiola *et al*., Nucl. Phys. **A583**, 119 (1995).
[18] F. Amorini, M. Cabibbo, G. Cardella, A. Di Pietro, P. Figuera, A. Musumarra, M. Papa, G. Pappalardo, F. Rizzo, and S. Tudisco, Phys. Rev. C **58**, 987 (1998).
[19] M. Papa, F. Amorini, M. Cabibbo, G. Cardella, A. Di Pietro, P. Figuera, A. Musumarra, G. Pappalardo, F. Rizzo, and S. Tudisco, Eur. Phys. J. A **4**, 69 (1999).
[20] S. Tudisco *et al*., Europhys. Lett. **58**, 811 (2001).
[21] M. Papa *et al*., Phys. Rev. C **68**, 034606 (2003).
[22] D. Pierroutsakou *et al*., Eur. Phys. J. A **16**, 423 (2003).
[23] D. Pierroutsakou *et al*., Eur. Phys. J. A **17**, 71 (2003).
[24] F. Amorini *et al*., Phys. Rev. C **69**, 014608 (2004).
[25] M. Papa *et al*., Phys. Rev. C **72**, 064608 (2005).
[26] W. D. Myers, W. J. Swiatecki, T. Kodama, L. J. El-Jaick, and E. R. Hilf, Phys. Rev. C **15**, 2032 (1977).
[27] W. D. Myers and W. J. Swiatecki, Ann. Phys. (NY) **84**, 186 (1973).
[28] M. Papa, T. Maruyama, and A. Bonasera, Phys. Rev. C **64**, 024612 (2001); M. Papa, G. Giuliani, and A. Bonasera, J. Comput. Phys. **208**, 403 (2005).
[29] M. Prakash, T. L. Ainsworth, and J. M. Lattimer, Phys. Rev. Lett. C **61**, 2518 (1988).
[30] J. D. Jakson, *Classical Electrodynamics* (Wiley, New York, 1962).